Sea ice diatom contributions to Holocene nutrient utilization in East Antarctica

Virginia Panizzo, Julien Crespin, Xavier Crosta, Aldo Shemesh, Guillaume Massé, Ruth Yam, Nadine Mattielli, Damien Cardinal

AGU PUBLICATIONS

Paleoceanography

CURRENTS

10.1002/2014PA002609

Key Points:
- A decoupling in nutrient utilization proxies occurs in the Neoglacial
- Sea-ice derived diatoms are discussed as a potential explanatory factor
- A departure from the application of nutrient proxies is discussed

Supporting Information:
- Tables S1 and S2

Correspondence to:
V. Panizzo,
virginia.panizzo@nottingham.ac.uk

Citation:
Panizzo, V., J. Crespin, X. Crosta, A. Shemesh, G. Massé, R. Yam, N. Mattielli, and D. Cardinal (2014), Sea ice diatom contributions to Holocene nutrient utilization in East Antarctica, *Paleoceanography*, *29*, 328–342, doi:10.1002/2014PA002609.

Received 14 JAN 2014
Accepted 5 MAR 2014
Accepted article online 21 MAR 2014
Published online 22 APR 2014

Sea ice diatom contributions to Holocene nutrient utilization in East Antarctica

Virginia Panizzo[1], Julien Crespin[2], Xavier Crosta[3], Aldo Shemesh[2], Guillaume Massé[4,5], Ruth Yam[2], Nadine Mattielli[6], and Damien Cardinal[5,6,7]

[1]Now at the School of Geography, University of Nottingham, Nottingham, UK, [2]Department of Earth and Planetary Sciences, Weizmann Institute of Science, Rehovot, Israel, [3]UMR-CNRS 5805 EPOC, Université Bordeaux I, Talence, France, [4]UMI 3376 TAKUVIK, CNRS and Université Laval, Québec, Quebec, Canada, [5]LOCEAN – IPSL, UPMC/IRD/CNRS/MNHN, Université Pierre et Marie Curie, Paris, France, [6]Laboratoire G-Time, Department of Earth and Environmental Sciences, Université Libre de Bruxelles, Bruxelles, Belgium, [7]Section of Mineralogy and Geochemistry, Royal Museum for Central Africa, Tervuren, Belgium

Abstract Combined high-resolution Holocene $\delta^{30}Si_{diat}$ and $\delta^{13}C_{diat}$ paleorecords are presented from the Seasonal Ice Zone, East Antarctica. Both data sets reflect periods of increased nutrient utilization by diatoms during the Hypsithermal period (circa 7800 to 3500 calendar years (cal years) B.P.), coincident with a higher abundance of open water diatom species (*Fragilariopsis kerguelensis*), increased biogenic silica productivity (%BSi), and higher regional summer temperatures. The Neoglacial period (after circa 3500 cal years B.P.) is reflected by an increase in sea ice indicative species (*Fragilariopsis curta* and *Fragilariopsis cylindrus*, up to 50%) along with a decrease in %BSi and $\delta^{13}C_{diat}$ ($< -18‰$ to $-23‰$). However, over this period, $\delta^{30}Si_{diat}$ data show an increasing trend, to some of the highest values in the Holocene record (average of +0.43‰). Competing hypotheses are discussed to account for the decoupling trend in utilization proxies including iron fertilization, species-dependent fractionation effects, and diatom habitats. Based on mass balance calculations, we highlight that diatom species derived from the semi-enclosed sea ice environment may have a confounding effect upon $\delta^{30}Si_{downcore}$ compositions of the seasonal sea ice zone. A diatom composition, with approximately 28% of biogenic silica derived from the sea ice environment (diat-SI) can account for the increased average composition of $\delta^{30}Si_{diat}$ during the Neoglacial. These data highlight the significant role sea ice diatoms can play with relation to their export in sediment records, which has implications on productivity reconstructions from the seasonal ice zone.

1. Introduction

Coastal and continental shelf zones are some of the most ecologically productive regions of the Southern Ocean (SO), accounting for up to approximately 76% and 3.5% of the total primary productivity of the marginal ice zone and SO, respectively [*Arrigo et al*., 2008; *Nelson et al*., 1995; *Smith and Gordon*, 1997]. Diatoms account for a large proportion of primary productivity in these regions, therefore dominating the biogeochemical cycling of silicon and strongly influencing the biogeochemical cycles of other macronutrients (e.g., nitrogen, carbon, and phosphorous) [*Sarmiento et al*., 2004].

The isotopic signature of silicon (Si) and carbon (C), which are preserved in the biogenic opal of diatoms ($\delta^{30}Si_{diat}$ and $\delta^{13}C_{diat}$, respectively), can be measured to reconstruct nutrient utilization and export production, providing an important link in understanding the role of the siliceous biological pump in transferring carbon into the deep ocean and regulating atmospheric concentrations of CO_2 over glacial-interglacial cycles (*De La Rocha et al*. [1997, 1998] and *Singer and Shemesh* [1995], respectively). Diatoms are dependent upon silicic acid ($Si(OH)_4$) within waters in order to form their opal frustules. These organisms biologically discriminate against the heavier ^{30}Si isotope relative to ^{28}Si, with a fractionation factor (ε) between waters and the organism, estimated in the SO of $-1.2 \pm 0.2‰$ [*Fripiat et al*., 2011]. *Varela et al*. [2004] also report a ε of $-1.2 \pm 0.1‰$, based on closed system mass balance modeling. Residual $Si(OH)_4$ in surface waters ($\delta^{30}Si_{Si(OH)4}$) retains a higher $\delta^{30}Si$ value. The degree, nature, and source of nutrient replenishment (e.g., open versus closed system Rayleigh models), strength of surface water stratification, and overall duration of growing seasons will all have important effects upon the composition of $\delta^{30}Si_{Si(OH)4}$ and therefore subsequent $\delta^{30}Si_{diat}$ signatures. In the same way, diatoms biologically discriminate against the heavier ^{13}C

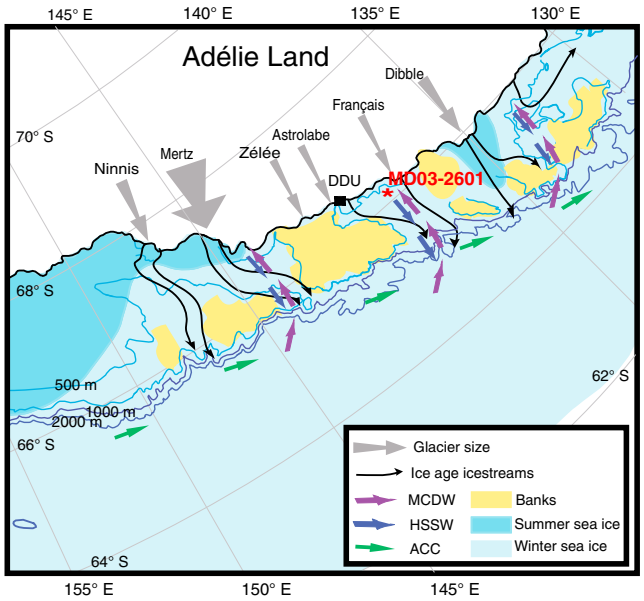

Figure 1. Site location in the SIZ, Adélie Land, East Antarctica. Core MD03-2601 is highlighted with a red asterisk. The presence of winter and summer sea ice is delimited along with regional glaciers, shallow bank areas, and dominant oceanic currents. Please refer to inset key for more information, where MCDW is Modified Circumpolar Deep Water; HSSW is High-Salinity Shelf Water; ACC is Antarctic Coastal Current; note that DDU refers to the Dumont d'Urville Trough. Image derived from *Crosta et al.* [2007].

isotope relative to ^{12}C. Variations in $\delta^{13}C_{diat}$ are attributed to changes in primary production, $[CO_2](aq)$ and sea ice coverage, as a large extent of sea ice reduces the outgassing of CO_2 from upwelled waters and induces depleted $\delta^{13}C_{diat}$ during diatom blooms [*Crosta and Shemesh*, 2002; *Rosenthal et al.*, 2000; *Schneider-Mor et al.*, 2005, 2008; *Shemesh et al.*, 1993].

To this date, only a handful of $\delta^{30}Si_{diat}$ studies [*De La Rocha et al.*, 1998; *Horn et al.*, 2011] and a relatively small number of $\delta^{13}C_{diat}$ studies exist from the SO [*Crosta and Shemesh*, 2002; *Crosta et al.*, 2002; *Hodell et al.*, 2001; *Jacot Des Combes et al.*, 2008; *Schneider-Mor et al.*, 2005; *Shemesh et al.*, 2002], all of them focusing on glacial-interglacial changes around the present Antarctic polar front, mostly in the Atlantic sector. To our knowledge, only one study was performed in the Antarctic coastal zone, where heavy sea ice conditions prevail for most of the year, which indicated that processes related to surface water mixing and stratification, as well as the structure of the whole water column, are important controls upon $\delta^{13}C_{diat}$ composition [*Berg et al.*, 2013]. There thus remains an absence of data that address the role that sea ice (SI) diatom communities may impart upon the sediment record, which is of great importance in the seasonal ice zone (SIZ) of the SO. Indeed, the presence of sea ice can hinder surface wind mixing and promote surface mixed layer (ML) stratification following spring melt. More recently, the focus on this closed (or at least semi-enclosed) sea ice environment has been highlighted for silicon isotopes [*Fripiat et al.*, 2007]. Here the progressive enrichment of the $\delta^{30}Si_{Si(OH)4}$ pool is pronounced, due to reduced nutrient exchange with surface waters [*Thomas and Papadimitriou*, 2003], which imparts a heavier sea ice diatom $\delta^{30}Si$ ($\delta^{30}Si_{diat\text{-}SI}$) signature (up to 1‰) than ML ($\delta^{30}Si_{diat\text{-}ML}$) counterparts [*Fripiat et al.*, 2007]. This manuscript provides a detailed investigation into the combined silicon and carbon pumps in the SIZ of East Antarctica, over the Holocene, by providing a high-resolution reconstruction of both $\delta^{30}Si_{diat}$ and $\delta^{13}C_{diat}$ on the same record from Adélie Land.

2. Site Description

Core MD03-2601 was collected in 2003 during the Images X cruise, aboard the R/V *Marion Dufresne II*, at 66°03.07'S, 138°33.43'E, in Adélie Land, East Antarctica. It was retrieved from a water depth of 746 m in one of the small depressions of the Dumont D'Urville Trough (DDUT) (Figure 1), a high accumulation site from the coastal and continental shelf zone (CCSZ). Today, $Si(OH)_4$ concentrations of the SIZ ML, in this region, are between 40 and 60 μmol/L in austral summer months (January–March), nitrate between 25 and 28 μmol/L

and phosphate <2 μmol/L (data from World Ocean Atlas). Indeed, austral spring (December) data published by *Cardinal et al.* [2007] also demonstrate initial (start of growing season) $Si(OH)_4$ ML values, in the SIZ at 64.9°S, of approximately 60 to 72 μmol/L with concentrations of BSi (<0.4 μm) at 0.40 μmol/L.

As outlined in *Crosta et al.* [2005], the trough has an average depth of 600–700 m, with the depressions acting to focus sedimenting phytoplankton cells (mainly diatoms) and thereby permitting good preservation of valves [*Wright and van den Enden*, 2000]. At the present time, sea ice covers the core site for 7–9 months of the year from February/March to November/December [*Arrigo and van Dijken*, 2003; *Schweitzer*, 1995]. The CCSZ is believed to be macronutrient and micronutrient rich, and ice melting produces a stratified stable environment favorable for diatom blooms [*Leventer*, 1992].

The data presented in this paper add to published work on sea-surface temperature, sea ice cover, and productivity changes [*Crosta et al.*, 2007, 2008; *Denis et al.*, 2006, 2009a, 2009b, 2010]. The main driver for the addition of $\delta^{30}Si_{diat}$ and $\delta^{13}C_{diat}$ analyses is to quantify specific nutrient utilization by diatoms (which dominate productivity in this region) over the Holocene. So far, proxies of productivity for this core include $\delta^{15}N_{bulk}$ and $\delta^{13}C_{bulk}$, both of which are subject to greater diagenetic changes compared to analyses conducted on diatom opal [*Anderson et al.*, 1998; *Crosta and Shemesh*, 2002; *Pondaven et al.*, 2000; *Singer and Shemesh*, 1995]. This multiproxy approach is therefore of great value to understand the numerous processes playing a role in this region during the Holocene.

3. Methods

3.1. Sediment Core and Chronology

The core itself is composed of diatomaceous ooze, alternating between structureless green ooze and green to dark green laminations (of millimeter to centimeter thickness) [*Crosta et al.*, 2005]. The age model used has been derived and extensively discussed by *Denis et al.* [2009a]. It is based on seven humic fraction (and one calcite shells and fragments fraction) ^{14}C dates, corrected with a 1300 year reservoir age [*Ingolfsson et al.*, 1998] and calibrated using CALIB 5.0 [*Stuiver et al.*, 2005] and the marine calibration Marine04 [*Hughen et al.*, 2004]. It should be noted that the carbonate fraction ^{14}C date may be up to 400 years younger than the surrounding humic fraction dates [*Costa et al.*, 2007]. We believe that it is, however, speculative to correct humic acid dates by 400 years. As this paper focuses on biogeochemical processes, we additionally state that correcting the MD03-2601 core chronology would not change our results and interpretations. We therefore choose to use the published chronology that indicates that the 40 m core covers the period between 1000 and 11,000 calendar years B.P. (cal years B.P.), with a mean sedimentation rate of 0.4 cm yr^{-1} [*Denis et al.*, 2006, 2009a].

3.2. Sample Cleaning for Stable Isotope Analyses of Diatom Opal

Between 5 and 8 g (depending on the amount of material available) of wet sediment (sampled at an interval of every 96 cm for $\delta^{30}Si_{diat}$ and every 32 cm for $\delta^{13}C_{diat}$) were prepared for isotopic analyses. A total of 58 samples were analyzed for $\delta^{30}Si_{diat}$ and 118 samples for $\delta^{13}C_{diat}$ from the core MD03-2601. In order to establish that cleaning techniques were reproducible and effective at both institutes, 17 additional cleaned subsamples (from the Weizmann Institute) from core MD03-2601 were sent to Université Libre de Bruxelles (ULB) for $\delta^{30}Si_{diat}$ analyses to also be conducted on the same samples. Note that these samples represent the only samples analyzed for both $\delta^{13}C_{diat}$ and $\delta^{30}Si_{diat}$.

Cleaning techniques are largely adapted from previously published diatom cleaning methods, in order to suit individual samples [e.g., *Juillet-Leclerc and Labeyrie*, 1987; *Morley et al.*, 2004; *Shemesh et al.*, 1995]. This involved stepwise cleaning of samples by wet sieving (between 10 and 32 μm size fractions) to remove larger nondiatom silicified organisms (e.g., radiolarian and sponge spicules). This fraction retained the dominant species assemblages of the core including the small Fragilariod taxa *Fragilariopsis curta*. Heavy density separation of samples using sodium polytungstate (Sometu Europa) at a specific gravity between 2.25 and 2.3 (adjusted to suit individual samples) was conducted a minimum of 3 times to remove lithogenic particles and clays. Carbonate removal (10% HCl for 2 h at room temperature) followed and organic digestion (a total of 4 h in 70% H_2O_2 at 65°C and 1 h at room temperature in 1:1 nitric:perchloric acid) was also conducted after which samples were washed and centrifuged in Milli Q water 8 times. Light microscopy and scanning electron

microscopy (SEM) confirmed good preservation of diatoms (e.g., minimal evidence of dissolution) and minimal contamination (Figure 2).

3.3. Silicon Isotopes

3.3.1. Alkaline Dissolution

All laboratory methods and analyses for this proxy were conducted at the ULB and the Royal Museum of Central Africa (Belgium). Samples were dried at 60°C in an oven before dissolution to liquid. Sealed Teflon Savillex pots were placed in a 100°C oven for approximately 70 min, with 1 mg of purified diatom opal and a 5 mL 0.2 M NaOH (Merck Pro Analysis) solution. Once dissolved, samples were immediately diluted (5 mL Milli Q) and acidified to neutralize the reaction with 5 mL 0.2 M HCl. Inductively coupled plasma–mass spectrometry (ICP-MS) analyses followed to ensure that lithogenic silica contamination (estimated from Al and Ti contents) was $< 1\%$. A known concentration of sample was passed through cationic resin (BioRad AG50W-X12), with 3 mL Milli Q elutant in order to obtain an optimal Si concentration (between 3 and 4 ppm Si) [*Georg et al*., 2006]. ICP-MS analyses were again conducted to ensure removal of all cations (e.g., Na^+) and establish final concentrations of Si in order to concentration match sample and bracketing standards.

3.3.2. Multi-Collector–Inductively Coupled Plasma–Mass Spectrometry (MC-ICP-MS) Analytical Methods

Silicon isotopes were analyzed on a Nu Plasma multi-collector–inductively coupled plasma–mass spectrometry (MC-ICP-MS) (Laboratoire G-Time of the Université Libre de Bruxelles, Belgium) using dry plasma mode with an Aridus II dessolvater. Stable isotope ratios of silicon are reported on a per mille (‰) basis ($\delta^{30}Si = ([(^{30}Si/^{28}Si)_{sample}/(^{30}Si/^{28}Si)_{std}] - 1) \times 1000]$), relative to the international Si sand standard NBS28 (National Institute of Standard and Technology, RM8546). Mass bias was corrected by external normalization, i.e., doping of samples with Mg [*Cardinal et al*., 2003], and Si and Mg concentration matching was adopted in samples and all standards. Long-term instrumental drift was also corrected by the sample-standard bracketing method, relative to NBS28. In order to resolve isobaric interference ($^{14}N^{16}O$) on ^{30}Si, pseudo high resolution was applied, setting analyses on the interference free left side of the peak (following methods outlined by *Abraham et al*. [2008]). Blank levels were monitored on ^{28}Si and were typically 50 to 100 mV, compared to a sample ^{28}Si signal of around 5 V. Blanks were not subtracted but such blank levels were found to be insignificant on replicates and secondary reference materials. Indeed, full and analytical replicates ($n \geq 3$) were conducted on all samples over several months, and results were compared to a known secondary reference, "Diatomite," with an analytical reproducibility for $\delta^{30}Si$ of +1.27‰ ± 0.18‰ ($1\sigma_{SD}$, $n = 84$) (published value of +1.26‰ ± 0.1‰ $1\sigma_{SD}$ [*Reynolds et al*., 2007]). $\delta^{29}Si$:$\delta^{30}Si$ ratios of all data were compared with the terrestrial fractionation line (1.96), and data points falling outside of its analytical error were excluded from final data (16 analyses out of the total number of analyses, $n = 341$).

3.4. Carbon Isotopes

All laboratory methods and analyses for this proxy were conducted at the Weizmann Institute, Israel. The carbon isotopic composition ($\delta^{13}C_{diat}$) and C content of diatom silica ($\%C_{diat}$) of the intrinsic organic matter encased within the cleaned diatom opal were analyzed on 118 samples using a Carlo Erba EA1110 elemental analyser in line with a Finnigan MAT 252 stable isotope ratio mass spectrometer. At least two replicates were measured for each sample. The $\delta^{13}C_{diat}$ values are reported versus peedee belemnite (PDB). Elemental analyzer runs were checked for internal consistency using several calibrated laboratory standards (acetanilide, glycine, and cellulose). As sampling resolution of biogenic silica (BSi) records [*Denis et al*., 2009b] and $\%C_{diat}$ were different, data points were interpolated for $\%C_{diat}$ so that ratios of %BiogenicSilica:$\%C_{diat}$ (%BSi:$\%C_{diat}$) could be calculated.

4. Results

4.1. Contemporary Nutrient Dynamics in the SIZ, East Antarctica

The range in diatom values reconstructed from core MD03-2601 ($\delta^{30}Si_{diat}$ between approximately −0.07 to +0.6‰) (Figures 3 and 4) fall close to the range of previously published values of $\delta^{29}Si_{BSi}$ from the SIZ region of Antarctica [*Cardinal et al*., 2007]. These values lie between −0.08 and +0.21‰ [*Cardinal et al*., 2007] for the ML (20–70 μm fraction at 63.9 and 64.9°S), which equates to $\delta^{30}Si_{BSi}$ values ranging between −0.16 and +0.41‰ (based on the kinetic isotopic fractionation factor of 1.96 to convert ^{29}Si into ^{30}Si which will be

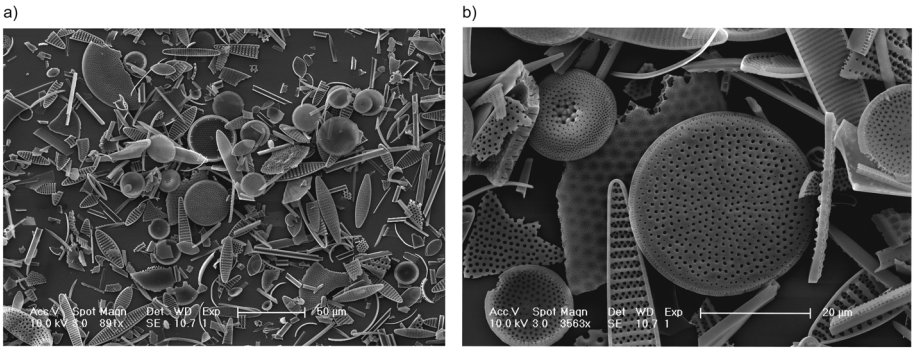

Figure 2. (a and b) SEM images showing the absence of lithogenic and organic particles in core samples of MD03-2601. Examples of samples used for stable isotope analyses of $\delta^{30}Si_{diat}$ and $\delta^{13}C_{diat}$.

applied to all respective data from hereinafter) [*Young et al*., 2002]. More recently, $\delta^{30}Si_{diat}$ values from sediment core tops taken from the Antarctic Peninsula (JCR112-BC383, 66.72°S and 70.44°W) have an average value of +0.9‰ [*Egan et al*., 2012]. This value is based on sediment fractions between the sizes 2 and 20 μm [*Egan et al*., 2012] where diatom composition is ≥ 90%. Measured $\delta^{30}Si_{Si(OH)4}$ values from site CTD124 (64.9°S) in the ML is +1.63 ± 0.11‰ (data from the CLIVAR SR3 transect between 140 and 144°E) [*Cardinal et al*., 2005]. When then applying the recent published fractionation factor estimate, based on a compilation of work from the SO of diatoms during uptake, $\varepsilon = -1.2‰ \pm 0.2‰$ [*Fripiat et al*., 2011], this provides a mean of $\delta^{30}Si_{diat}$ of +0.43 ± 0.23‰ ($1\sigma_{SD}$) (assuming that initial waters are in equilibrium). Again within the range of those reconstructed from core MD03-2601, supporting the application of the technique to reconstruct Holocene utilization in this region.

Absolute $\delta^{13}C_{diat}$ values from core MD03-2601 range between −23.5 and −17.8‰, which are in the range of values expected for the SO during the Holocene, between −17 and −25‰ [*Berg et al*., 2013; *Crosta and Shemesh*, 2002; *Crosta et al*., 2002; *Hodell et al*., 2001; *Jacot Des Combes et al*., 2008; *Schneider-Mor et al*., 2008; *Shemesh et al*., 2002]. Moreover, as already observed by *Berg et al*. [2013], the variability of the $\delta^{13}C_{diat}$ during the Holocene in the coastal zone is in the same order of magnitude as the one observed for glacial-interglacial changes (1–5‰) [*Crosta and Shemesh*, 2002; *Crosta et al*., 2002; *Jacot Des Combes et al*., 2008; *Rosenthal et al*., 2000; *Schneider-Mor et al*., 2005, 2008; *Shemesh et al*., 2002].

4.2. MD03-2601 Proxy Data

Contamination in all MD03-2601 samples analyzed for C and Si stable isotopes was minimal, with percent carbon content ranging between 0.15 and 0.29% and lithogenic Si content <1% (both Al:Si and Ti:Si < 1). As a result, cleaning methods applied at both Institutes were reproducible and robust. SEM imaging of samples clearly demonstrates this (Figures 2a and 2b). Reproducibility of stable isotope analyses yielded an average precision ($1\sigma_{SD}$) of ± 0.12‰ for $\delta^{30}Si_{diat}$, 0.09‰ for $\delta^{13}C_{diat}$, and 0.004% for %C. Please refer to supporting information Tables S1 and S2 for full $\delta^{30}Si_{diat}$ and $\delta^{13}C_{diat}$ data.

High values of $\delta^{30}Si_{diat}$ in the record are seen between circa 11,000 and circa 10,000 cal years B.P., fluctuating at approximately +0.57‰, after which values soon decline, until circa 7200 cal years B.P., fluctuating between approximately +0.35‰ and −0.07‰, the lowest values in the record (Figure 3c). The decreasing trend in $\delta^{30}Si_{diat}$ starting circa 10,000 cal years B.P. is concomitant with the decrease in species abundances of *Fragilariopsis kerguelensis* and sea ice indicative species (here total abundances of *F. curta* and *F. kerguelensis*) (Figures 3e and 3f). These changes are also coincident with an increase in %BSi:%C_{diat} (Figure 3a) reaching as high as circa 300 until circa 8500 cal years B.P. $\delta^{13}C_{diat}$ remains relatively stable, between circa 11,000 and 8000 cal years B.P., with values ranging between −19 and −22‰ (Figure 3b).

At circa 7800 and 7100 cal years B.P., values of $\delta^{13}C_{diat}$ and $\delta^{30}Si_{diat}$, respectively (Figures 3b and 3c), show an increase to higher values. $\delta^{13}C_{diat}$ increases to approximately −20‰ with highest values over this period reaching −18.5‰. This enrichment is seen until circa 3700 cal years B.P. $\delta^{30}Si_{diat}$ values between circa 7100

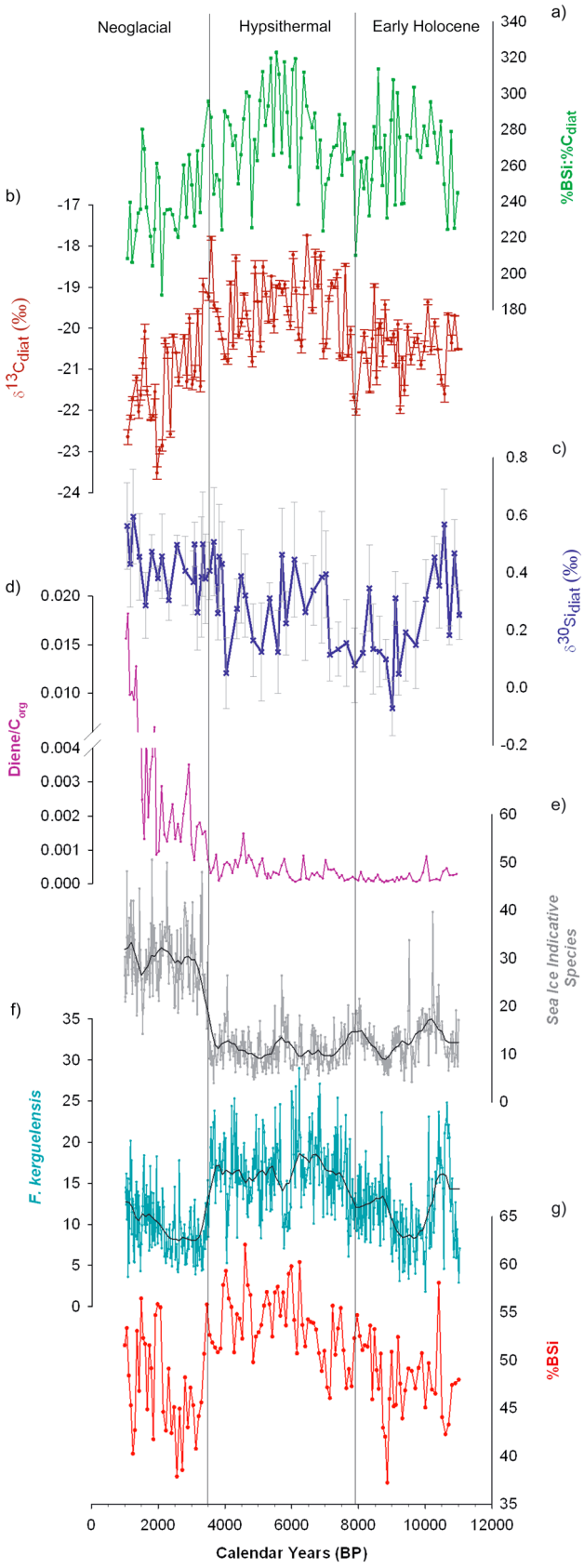

Figure 3

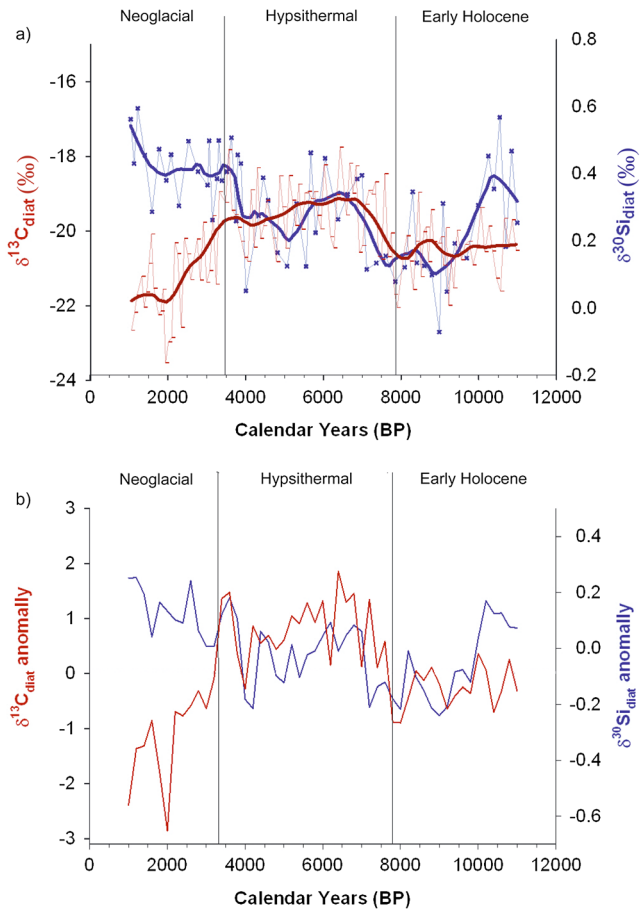

Figure 4. Down core records from MD03-2601 versus calendar years before present (cal years B.P.), (a) $\delta^{13}C_{diat}$ (‰) and $\delta^{30}Si_{diat}$ (‰) plotted together and a LOESS smooth is superimposed on both records to highlight main trends, and (b) normalized anomaly plots showing the deviation from the Holocene mean for both $\delta^{13}C_{diat}$ and $\delta^{30}Si_{diat}$ records. Black lines, for both plots, delimit the three periods discussed in the text.

and 3800 cal years B.P. vary between +0.05 and +0.46‰. The changes in these two proxies are concomitant with an increase in *F. kerguelensis* species abundances (Figure 3f) after circa 7500 cal years B.P. and increased %BSi (up to approximately 60%) after circa 7600 cal years B.P. %BSi:%C_{diat} increase once more after circa 7000 cal years B.P., reaching values as high as 320 (Figure 3a).

By 3800 cal years B.P., $\delta^{30}Si_{diat}$ values increase and fluctuate between +0.26‰ and +0.60‰ until the end of the record (Figure 4a). However, after circa 3500 cal years B.P., $\delta^{13}C_{diat}$ values show a decreasing trend to the lowest values in the record (Figures 3b and 4a). This change is concomitant with the increase in sea ice indicative species, increasing to average values of approximately 30% for the rest of the record (Figure 3e). After circa 3700 cal years B.P., %BSi shows a sharp decline (<50%) to some of the lowest values in the record before increasing again after circa 1500 cal years B.P. (Figure 3g). The %BSi:%C_{diat} ratio shows a decreasing trend after circa 4500 cal years B.P., reaching the lowest values seen in the record, although by circa 2100 cal years B.P. a small increase is seen (Figure 3a). A rapid increase is seen after circa 3800 cal years B.P. in Diene/C_{org} ratios (Diene data from *Denis et al.* [2010]), to the highest in the record (approximately 0.02) (Figure 3d).

Figure 3. Down core records from MD03-2601 versus calendar years before present (cal years B.P.), (a) %BSi:%C_{diat}, (b) $\delta^{13}C_{diat}$ (‰) and respective 1 standard deviation (SD) error bars in red, (c) $\delta^{30}Si_{diat}$ (‰) and respective 1 SD error bars in grey, (d) Diene/C_{org} ratios, (e) percentage abundances of sea ice indicative species (*F. curta* and *F. cylindrus*, with a three-point running average superimposed in black) (data from *Crosta et al.* [2008]), (f) percentage abundances of *F. kerguelensis* (with a three-point running average superimposed in black), (g) $\%BSi_{bulk}$. Black lines delimit the three periods discussed in the text.

5. Discussion

The Holocene record from core MD03-2601, presented here, has been divided into three periods (Figures 3 and 4). These follow the periods outlined by *Crosta et al.* [2008] and *Denis et al.* [2009b], based on high-resolution changes in dominant diatom assemblages and geochemical proxies over the course of the Holocene: the early Holocene (circa 11,000 to 7800 cal years B.P.), the mid-Holocene Hypsithermal (circa 7800 to circa 3500 cal years B.P.), and the late Holocene Neoglacial (circa 3500 to circa 1000 cal years B.P.). It is worth noting that the resolution of the new data sets presented here does not permit centennial-to-millennial oscillations to be discussed [*Denis et al.*, 2009b].

5.1. Early- to Mid-Holocene Productivity Changes

High values of $\delta^{30}Si_{diat}$ are encountered during 11,000 cal years B.P. to 10,000 cal years B.P., followed by lower values until 7700 cal years B.P., while $\delta^{13}C_{diat}$ data presents values around −20.5‰ during the whole early Holocene. Antarctic ice core records document that the early Holocene (11,000 to 9000 cal years B.P.) represents the warmest period of the Holocene in East Antarctica [*Masson et al.*, 2000]. This is indeed reflected by the higher abundances of the open water (e.g., summer) diatom species *F. kerguelensis* (between circa 11,000 and 10,000 cal years B.P.; Figure 3f), which are in phase with the $\delta^{30}Si_{diat}$ pattern during the early Holocene. *Fragilariopsis kerguelensis* is a strongly silicified species [*Gall et al.*, 2001; *Scharek et al.*, 1997; *Takeda*, 1998], which has a preferentially higher $Si(OH)_4$ demand compared to more weakly silicified diatom species [*Smetacek*, 1998]. The overwhelming abundances of *F. kerguelensis* between circa 11,000 and 10,000 cal years B.P. may explain the high %BSi:$\%C_{diat}$ values at that time (Figure 3a).

The later decline in $\delta^{30}Si_{diat}$ is concomitant with a documented Antarctic cooling (up to 1°C) between circa 10,000 and 8000 cal years B.P. [*Mathiot et al.*, 2013]. In the region of East Antarctica, this is reflected as sea ice expansion and glacial advances, as suggested by higher relative abundances of *F. curta*, and greater surface water stratification, as demonstrated by higher abundances of *Chaetoceros* resting spores (CRS) [*Crosta et al.*, 2008; *Denis et al.*, 2009a]. High surface water stratification most likely induced early season depletion of other nutrients (e.g. nitrate) prior to silicic acid [*Denis et al.*, 2009b] but overall low productivity at the time, thereby leading to low Si utilization by diatoms and therefore lower $\delta^{30}Si_{diat}$.

The initiation of the Hypsithermal is clearly identified in core MD03-2601 between circa 7800 cal years B.P. and circa 3500 cal years B.P. during which period %BSi was above 50% (Figure 3g). Centennial timescale episodes of maximum productivity were recorded at circa 7000, 6000, and 4000 cal years B.P. [*Denis et al.*, 2009b]. Both millennial and centennial timescale changes are coincident with increased abundances of the heavily silicified, open water species *F. kerguelensis*. More specifically, %BSi:$\%C_{diat}$ ratios also increases after circa 7000 cal years B.P. to the highest values seen in the record (Figure 3a). These data suggest a preferential increase in silicic acid utilization over carbon utilization, driving the higher composition of $\delta^{30}Si_{diat}$ during the Hypsithermal (between approximately +0.05‰ and approximately +0.46‰).

With regard to the $\delta^{13}C_{diat}$ record, as previously outlined for the open ocean, variations in $\delta^{13}C_{diat}$ are attributed to changes in primary production, $[CO_2](aq)$ and sea ice coverage, as a large extent of sea ice reduces outgassing of CO_2 from upwelled waters and induces depleted $\delta^{13}C_{diat}$ during diatom blooms [*Crosta and Shemesh*, 2002; *Rosenthal et al.*, 2000; *Schneider-Mor et al.*, 2005, 2008; *Shemesh et al.*, 1993]. So far, only one study presents Holocene $\delta^{13}C_{diat}$ values from the SIZ, which range between −26‰ and −20‰ [*Berg et al.*, 2013], comparable to our $\delta^{13}C_{diat}$ results. However, literature on particulate organic matter and particulate organic carbon ($\delta^{13}C_{POM}$ and $\delta^{13}C_{POC}$, respectively) within sea ice does exist, showing values ranging between approximately −30.5‰ and −8‰ [*Arrigo et al.*, 2003; *Gibson et al.*, 1999; *McMinn et al.*, 1999; *Michels et al.*, 2008; *Munro et al.*, 2010]. This large range of $\delta^{13}C_{POM}$ and $\delta^{13}C_{POC}$ values within sea ice is not discriminating and cannot explain our data. However, a positive relationship has been found between phytoplanktonic productivity and $\delta^{13}C_{POC}$ in the Ross Sea [*Villinski et al.*, 2000]. We therefore argue that the high $\delta^{13}C_{diat}$ values observed during the Hypsithermal are due to an increase in total dissolved inorganic carbon (DIC) utilization (i.e., higher productivity). A result of increased productivity, decreased sea ice season duration, reduced stratification of the water column [*Crosta et al.*, 2008; *Denis et al.*, 2009b, 2010; *Kim et al.*, 2012], and warm atmospheric temperatures over East Antarctica [*Masson et al.*, 2000; *Masson-Delmotte et al.*, 2004].

5.2. Late Holocene Nutrient Decoupling

After circa 3600 cal years B.P., there is a distinct change in proxy records (Figure 3) whereby both carbon and silicon isotope trends are decoupled (Figures 4a and 4b). After circa 3800 cal years B.P., we observe a sharp $\delta^{30}Si_{diat}$ increase in our record (ranging between approximately +0.26‰ and approximately + 0.60‰), suggesting a period of increased $Si(OH)_4$ utilization by diatoms (Figure 3c) during the Neoglacial. In contrast, from circa 3600 cal years B.P., $\delta^{13}C_{diat}$ values are gradually decreasing to reach the lowest values of the records (approximately −23‰) by 2000 cal years B.P. (Figure 3b). These changes are more evident in Figures 4a and 4b where an opposing trend in isotopic proxies is seen, particularly when considering Figure 4b which displays the deviation from the record mean of both proxies therefore emphasizing the divergence in records. In the following section, we will outline possible mechanisms that could be explaining these contradicting trends in our record and highlight the potential implications for paleoreconstructions.

Initial calculations of ε (−1.1 ± 0.4‰) [*De La Rocha et al*., 1997] were determined based on laboratory experiments of dominant temperate/subpolar marine diatoms species, under a closed system model (e.g., progressive enrichment in ^{30}Si of the source pool, with increased utilization). Results showed that ε did not statistically vary between cultured species, and it was insensitive to growth rate and the temperature of source waters (from 12°C to 22°C) [*De La Rocha et al*., 1997] as well as Si quotas and the pCO_2 concentrations of waters [*Milligan et al*., 2004]. However, comparisons between different studies did show slight differences in ε for certain cultured species (e.g., *Thalassiosira weissflogii*) [cf. *De La Rocha et al*., 1997; *Milligan et al*., 2004]. More recent literature has argued that ε may indeed show a species-dependent fractionation effect [*Sutton et al*., 2013]. Through laboratory culturing of a number of dominant polar and subpolar diatom strains, *Sutton et al*. [2013] indeed propose that SO species display the widest range in ε (e.g., −0.54 ± 0.09‰ for *F. kerguelensis* and −2.09 ± 0.09‰ for *Chaetoceros brevis*) [*Sutton et al*., 2013]. These species-dependent fractionation effects highlighted may indeed provide a plausible explanation since, *F. kerguelensis*, one of the diatom strains cultured by *Sutton et al*. [2013], presents strong changes in relative and absolute abundances in core MD03-2601. However, the smaller fractionation factor (ε) of −0.54 ± 0.09‰ (compared to −1.2 ± 0.2‰, estimated from a compilation of in situ SO measurements) [*Fripiat et al*., 2011] suggest that the highest $\delta^{30}Si_{diat}$ values would dominate during periods when *F. kerguelensis*is are the most abundant (e.g., during the Hypsithermal; Figures 3c and 3f), which is opposite to the trend observed in our record. It is therefore highly unlikely that the species effect observed by Sutton and coworkers can explain the increasing trend observed in our record during the Neoglacial period, when sea ice indicative species dominate (Figures 3c and 3d). While *Sutton et al*. [2013] highlight the need to further constrain any evidence of species-dependent fractionation effects, until this is further elucidated, we apply the average silicon isotope fractionation factor more recently published by *Fripiat et al*. [2011].

A second potential explanation for the opposite trends in diatom utilization of silicon and carbon during the Neoglacial (Figures 4a and 4b), could be iron (Fe), as in the context of the SO, Fe (bio-)availability may also play a considerable role upon silicon utilization. In certain regions of the ocean, Fe is regarded as a limited nutrient for diatoms, (e.g., the High Nitrate, Low Chlorophyll (HNLC) regions) and during periods of increased (bio-)availability (e.g., enhanced aeolian transport in glacial periods) [*Brzezinski et al*., 2003], there is a documented increase in diatom productivity [*Boyd et al*., 2000; *Brzezinski et al*., 2003; *Martin and Fitzwater*, 1988; *Martin and Gordon*, 1988; *Martin et al*., 1990a, 1990b]. *Brzezinski et al*. [2003] clearly describe that during Fe-limited conditions (e.g., interglacial periods) in HNLC regions, diatoms utilize silicon and nitrate ($Si(OH)_4$:NO_3^-) with a depletion ratio >4:1, while during Fe replete conditions (e.g., glacial periods), this ratio changes to a more normal 1:1 ratio [*Brzezinski*, 1985]. These shifts are believed to account for pCO_2 drawdown during glacial periods when aeolian sources of Fe increased, promoting $Si(OH)_4$ export to lower latitudes and enhancing the silica and carbon biological pumps in regions where the carbonate production would once have dominated [e.g., *Arellano-Torres et al*., 2011; *Beucher et al*., 2007; *Matsumoto et al*., 2002; *Pichevin et al*., 2012].

Coastal and shelf waters of the SO are generally considered to be highly productive regions due to the Fe inputs from underlying sediments and land runoff [*Martin*, 1990; *Smetacek et al*., 2004]. Extensive work in polynya regions of the Amundsen Sea have argued that sea ice and Pine Island glacial meltwater can play a significant role in providing bioavailable Fe, thereby promoting phytoplankton growth in continental regions of the SO [*Alderkamp et al*., 2012; *Mills et al*., 2012]. Indeed, *Thuróczy et al*. [2012] also document that upwelling

nutrient-rich Modified Circumpolar Deep Water, and unsaturated organic ligands, are important sources of Fe in the Amundsen Sea. Indeed, the latter is able to further fuel phytoplankton blooms in this polynya region due their ability to stabilize additional Fe derived from glacial meltwaters, in turn further aiding the solubilization of Fe. These data suggest that in the modern day, the Amundsen Region of the SO is Fe replete. In the Western Antarctic Peninsula, *Weston et al*. [2013] also document high overall primary productivity, a result of high dissolved bioavailable Fe [*Ardelan et al*., 2010], particularly in Marguerite Bay due to glacial meltwater inputs to the region. While *Sambrotto et al*. [2003] argue that the Upper Circumpolar Deep Water, upwelling in the region of Adélie Land, East Antarctica, is a valuable source of bioavailable Fe, their results do not clearly conclude whether seasonal nutrient drawdown is simply a result of continued diatom-dominated growth or Fe limitation in the region. Furthermore, in the Ross Sea, *Sedwick et al*. [2000] also documented trace metal (Fe and Manganese) depletion ($<$ 0.2 nM DFe) and therefore Fe limitation of phytoplankton during summer months. The authors [*Sedwick et al*., 2000] highlight the great spatial and temporal variability that exists in biogeochemical cycling, due to the complex interplay of coastal processes at different stages of the year (e.g., upwelling, glacial meltwater inputs, and sea ice cover) [*Arrigo et al*., 1998]. Nevertheless, in the modern day, it would appear that the SIZ of the SO, particularly in polynya regions is, in general, a Fe replete environment and the nutrient was most likely not limiting over the Holocene.

A final explanation to account for the deviation in nutrient trends over the Holocene resides in diatom habitats (Figures 4a and 4b). Monitoring data of assemblages within the SIZ in East Antarctica have shown that *F. curta* and *F. cylindrus* are not only able to thrive under the ice but also multiply successfully within the ice [*Fiala et al*., 2006]. As such, *F. curta* cells growing within ice environments exhibit a heavier isotopic signature than their open ocean dwelling counterparts (up to approximately +1‰ more) [*Fripiat et al*., 2007]. This is resulting from the growth of cells in a semi-enclosed system where the dissolved silicon pool (i.e., brine) is only partially replenished [*Fripiat et al*., 2007]. Studies looking at the compositional changes of sea ice brines in the Weddell Sea have indeed shown a $Si(OH)_4$ drawdown by resident diatom populations over the course of the austral summer [*Papadimitriou et al*., 2007]. As such, the concomitant increase in sea ice indicative species and $\delta^{30}Si_{diat}$ in the Neoglacial period (Figures 3e and 3c, respectively) could reflect the increased contribution of sea ice-derived species (hereafter referred to as diat-SI) to the sediment, yielding a bulk higher relative utilization of the Si pool driven by Si limitation in sea ice habitats. Variations in relative abundances of diatom specific biomarkers, with, in particular higher relative abundance of a di-unsaturated Highly Branched Isoprenoidalkene (HBI Diene) after circa 4000 cal years B.P. (Figure 3d), also suggest a higher contribution of sea ice-derived diatoms to the sediment [*Denis et al*., 2010]. *Massé et al*. [2011] have shown that this isomer is unique to sea ice diatom communities and that high abundances of this biomarker are observed in sea ice-covered environments, with more recent studies further confirming the application of this proxy in the Southern Ocean [e.g., *Barbara et al*., 2013; *Collins et al*., 2013]. As such, it is highly likely that the decoupling between carbon and silicon proxies during the Neoglacial is driven by the increased proportion of diat-SI in core MD03-2601, which has a higher $\delta^{30}Si$ composition as a result of their semi-enclosed environment.

In order to investigate this argument further, we estimated the relative diat-SI contribution ($\%abundance_{diat\text{-}SI}$) relative to the diat-ML contribution ($\%abundance_{diat\text{-}ML}$) in MD03-2601 sediments using the following equation:

$$Fraction\_SI = \left(\delta^{30}Si_{downcore} - \delta^{30}Si_{diat\text{-}ML}\right) / \left(\delta^{30}Si_{diat\text{-}SI} - \delta^{30}Si_{diat\text{-}ML}\right),$$

where $\delta^{30}Si_{diat\text{-}SI}$ and $\delta^{30}Si_{diat\text{-}ML}$ values are +1.2‰ ± 0.24‰ [*Fripiat et al*., 2007] and +0.12‰ ± 0.28‰, respectively (based on data from *Cardinal et al*. [2007] and *Varela et al*. [2004]) and $\delta^{30}Si_{downcore}$ is the average $\delta^{30}Si_{diat}$ value (+0.43‰, ranging between +0.26‰ and +0.60‰) during the Neoglacial interval in core MD03-2601. We are able to propagate the errors on both the variability in the downcore data over the Neoglacial ($\delta^{30}Si_{downcore}$ = +0.43‰ ± 0.17‰) and of the published values of diat-SI and diat-ML, as detailed above, when making these calculations. Based on this, we argue that approximately 28 ± 31% of biogenic silica (BSi) preserved in core MD03-2601 in the Neoglacial, would need to be derived from diatoms thriving in the sea ice environment (diat-SI) to account for the higher isotopic composition of silicon, as an alternative interpretation to increased productivity at this time. Nevertheless, the consequences of the estimates from the Neoglacial suggest that either the export efficiency of these organisms is thus particularly efficient and/or the export from open water diatoms has been dramatically reduced at this period.

While the more extreme end-member calculations values are high, the percentage abundance of sea ice-related species in core MD03-2601 reach a maximum of approximately 50% over the Neoglacial period [*Crosta et al*., 2007, 2008] (Figure 3e). However, it should be noted that estimating the downcore variations in the abundance of ice-derived diatom cells is extremely difficult, since these populations can "seed" ice edge blooms [*Leventer*, 2003, and references therein; *Lizotte*, 2001]. Furthermore, bloom development will depend upon the stratification of the shallow ML and nutrient availability [*Arrigo and Thomas*, 2004]. Nevertheless, this argument identifies the complex role that sea ice plays and how, potentially, it can have a confounding impact on paleoarchives of past utilization.

Within sea ice, as already outlined in section 5.1., $\delta^{13}C_{POM}$ and $\delta^{13}C_{POC}$ show a very large range of values [*Arrigo et al*., 2003; *Gibson et al*., 1999; *McMinn et al*., 1999; *Michels et al*., 2008; *Munro et al*., 2010]. The highly variable nature of $\delta^{13}C$ in ice habitats was further confirmed by *Cozzi and Cantoni* [2011], who documented that $\delta^{13}C_{POC}$ values from fast ice (Terra Nova Bay) vary between approximately −30.7 and −15‰ and that a clear negative correlation ($r^2 = 0.94$) exists between POC and $\delta^{13}C_{POC}$ from the different ice layers. Interestingly, the lower values of $\delta^{13}C_{diat}$ in core MD03-2601 are inconsistent with the interpretation of depleted $[CO_2](aq)$ concentrations in the semi-closed sea ice environment, with continued diatom growth and nutrient depletion [e.g., *Gibson et al*., 1999; *Kennedy et al*., 2002; *Papadimitriou et al*., 2007, 2009; *Rau et al*., 1991; *Thomas et al*., 2001; *Thomas and Papadimitriou*, 2003]. However, *Kennedy et al*. [2002] document that $\delta^{13}C_{POC}$ for summer sea ice, ranges between −26.6‰ and −11.9‰ from continuous ice floes and −25.0‰ and −10.0‰ in layered ice floes, while average values of $\delta^{13}C_{POC}$ from seawater are −26.1‰ [*Kennedy et al*., 2002]. These ranges suggest little differentiation between the two environments. $\delta^{13}C_{diat}$ values after circa 3500 cal years B.P. in core MD03-2601 have an average of approximately −21.3‰ (ranging between −23.5‰ and −18.9‰), while average $\delta^{13}C_{bulk}$ [*Crosta et al*., 2005; *Denis et al*., 2009b] after this time averages at −25.9‰, capturing the ranges in published open water (or ice) [*Kennedy et al*., 2002] $\delta^{13}C_{POM}$ and $\delta^{13}C_{POC}$. Moreover, the recent study by *Berg et al*. [2013] showed high abundances (approximately 30–50%) of *F. curta* (sea ice-related diatoms) were associated with light $\delta^{13}C_{diat}$ values (ranging between approximately −26‰ and −20‰). These light values are in the range of $\delta^{13}C_{diat}$ values observed in core MD03-2601 during the Neoglacial, also coincident with high abundances of sea ice-derived species (Figures 3b, 3d, and 3e).

Thus, due to the large range in $\delta^{13}C$ values observed in the SO from different environments, we do not aim to quantify the changes in $\delta^{13}C_{diat}$ as a function of diat-SI and diat-ML populations in core MD03-2601. Rather we argue that low $\delta^{13}C_{diat}$ values observed in core MD03-2601 during the Neoglacial were due to a decrease in total dissolved inorganic carbon (DIC) utilization (i.e., lower productivity) and/or increased supply to the region (e.g., upwelling) over this period [*Denis et al*., 2009a; 2009b]. This is concomitant with cooler temperatures and prolonged sea ice cover [*Renssen et al*., 2005]. More precisely, the combination of greater sea ice cover reducing CO_2 outgassing and the effect of intensified upwelling may be able to account for the low $\delta^{13}C_{diat}$ at this time as both processes increase the DIC pool at the surface. However, we cannot exclude the possible explanation that the observed lighter $\delta^{13}C_{diat}$ values could also result from more intense POC recycling, within sea ice environments.

Undoubtedly, further research to constrain silicon cycling in ML and SI environments, and ultimately its export, is needed. However, this argument does highlight its potential for Neoglacial nutrient decoupling in core MD03-2601 (Figure 4). These findings have important implications when comparing utilization proxies from the SIZ as these data suggest a departure from the interpretation of $\delta^{30}Si$ as a utilization proxy of the ML if the contribution of diatoms originating from sea ice to the total sediment diatom record is not taken into account. Nevertheless, we show that on a high-resolution sediment core, Si isotopic data can be used to quantify the relative contribution of sea ice diatoms to the bulk biogenic silica record.

6. Conclusions

We present the highest resolution Holocene coupled $\delta^{30}Si_{diat}$ and $\delta^{13}C_{diat}$ records from the SIZ, East Antarctica. These data are compared with dominant diatom species assemblage changes, along with %BSi and %BSi:%C_{diat} ratios. There is a general agreement between carbon and silicon utilization proxies over the duration of the record until circa 3500 cal years B.P. During the Holocene Hypsithermal (between circa 7800 and circa 3500 cal years B.P.), $\delta^{13}C_{diat}$ and $\delta^{30}Si_{diat}$ increase, concomitant with increased percentage

abundances of open water diatom species (*F. kerguelensis*) and other diatom productivity proxies (e.g., %BSi and %BSi:%C_{diat}), probably a result of increased temperatures and a longer growing season in the region over this period. After circa 3500 cal years B.P., during the Neoglacial, opposite trends are seen in $\delta^{13}C_{diat}$ and $\delta^{30}Si_{diat}$. Several explanations are explored including species-dependent fractionation effects, Fe fertilization, and sea ice cover. However, we argue the increased representation (the mass balance calculation of approximately 28%BSi) of diatoms derived from sea ice environments (also supported by higher relative abundances of HBI Diene) could account for higher Neoglacial $\delta^{30}Si_{diat}$ downcore values, when other nutrient utilization proxies suggest reduced productivity. These data highlight a significant contribution of sea ice-derived material exported to the sediment when sea ice cover is extended. It has important implications for interpreting downcore productivity records in the SIZ of the SO and that a departure in the application of these proxies can occur when high abundances of sea ice-derived species are present. This works propose a comprehensive, multiproxy approach to elucidate these arguments further, in the future.

Acknowledgments

Virginia Panizzo conducted all $\delta^{30}Si_{diat}$ analyses at the Laboratory G-Time at the Université Libre de Bruxelles, Belgium. This work has been performed within the framework of the ESF HOLOCLIP Project, a joint research project of the European Science Foundation Polar CLIMATE program, funded by national contributions from Italy, France, Germany, Spain, Netherlands, Belgium, and United Kingdom. In Belgium, the support was provided by FNRS (FRFC 2.4534.10). This is HOLOCLIP contribution 23. Damien Cardinal has received funding from the European Union Seventh Framework Programme under grant agreement 294146 (Marie Curie CIG, MuSiCC). The authors would like to thank Luc André and Laurence Monin (RMCA) for their assistance and support during the project. The authors would also like to thank Christine Cocquyt at the National Botanic Garden of Belgium for the use of their Light Microscope facilities for this study. Figure 1 is reproduced with the permission of John Wiley & Sons, Inc. 2013.

References

Abraham, K., S. Opfergelt, F. Fripiat, A. J. Cavagna, J. T. M. de Jong, S. F. Foley, L. Andre, and D. Cardinal (2008), δ^{30}Si and δ^{29}Si determinations on USGS BHVO-1 and BHVO-2 reference material with a new configuration on a Nu Plasma Multi-Collector ICP-MS, *Geostand. Geoanal. Res.*, *32*(2), 193–202.

Alderkamp, A.-C., et al. (2012), Iron from melting glaciers fuels phytoplankton blooms in the Amundsen Sea (Southern Ocean): Phytoplankton characteristics and productivity, *Deep Sea Res., Part II*, *71-76*, 32–48, doi:10.1016/j.dsr2.2012.03.005.

Anderson, R. F., N. Kumar, R. A. Mortlock, P. N. Froelich, P. Kubik, B. Dittrich-Hannen, and M. Suter (1998), Late-Quaternary changes in productivity of the Southern Ocean, *J. Mar. Syst.*, *17*(1-4), 497–514, doi:10.1016/S0924-7963(98)00060-8.

Arellano-Torres, E., L. E. Pichevin, and R. S. Ganeshram (2011), High-resolution opal records from the eastern tropical Pacific provide evidence for silicic acid leakage from HNLC regions during glacial periods, *Quat. Sci. Rev.*, *30*(9-10), 1112–1121, doi:10.1016/J.Quascirev.2011.02.002.

Arrigo, K. R., and D. N. Thomas (2004), Large-scale importance of sea ice biology in the Southern Ocean, *Antarct. Sci.*, *16*(4), 471–486.

Arrigo, K. R., and G. L. van Dijken (2003), Phytoplankton dynamics within 37 Antarctic coastal polynya systems, *Geophys. Res. Lett.*, *108*(C8), 3271, doi:10.1029/2002JC001739.

Arrigo, K. R., A. M. Weiss, and W. O. Smith (1998), Physical forcing of phytoplankton dynamics in the southwestern Ross Sea, *J. Geophys. Res.*, *103*(C1), 1007–1021, doi:10.1029/97JC02326.

Arrigo, K. R., D. H. Robinson, R. B. Dunbar, A. R. Leventer, and M. P. Lizotte (2003), Physical control of chlorophyll *a*, POC, and TPN distributions in the pack ice of the Ross Sea, Antarctica, *J. Geophys. Res.*, *108*(C10), 3316, doi:10.1029/2001JC001138.

Arrigo, K. R., G. L. van Dijken, and S. Bushinsky (2008), Primary production in the Southern Ocean, 1997–2006, *J. Geophys. Res.*, *113*, C08004, doi:10.1029/2007JC004551.

Barbara, L., X. Crosta, S. Schmidt, and G. Massé (2013), Diatoms and biomarkers evidence for major changes in sea ice conditions prior the instrumental period in Antarctic Peninsula, *Quat. Sci. Rev.*, *79*(0), 99–110, doi:10.1016/j.quascirev.2013.07.021.

Berg, S., M. J. Leng, C. P. Kendrick, H. Cremer, and B. Wagner (2013), Bulk sediment and diatom silica carbon isotope composition from coastal marine sediments off East Antarctica, *Silicon*, *5*(1), 19–34, doi:10.1007/S12633-012-9113-3.

Beucher, C. P., M. A. Brzezinski, and X. Crosta (2007), Silicic acid dynamics in the glacial sub-Antarctic: Implications for the silicic acid leakage hypothesis, *Global Biogeochem. Cycles*, *21*, Gb3015, doi:10.1029/2006GB002746.

Boyd, P. W., et al. (2000), A mesoscale phytoplankton bloom in the polar Southern Ocean stimulated by iron fertilization, *Nature*, *407*(6805), 695–702.

Brzezinski, M. A. (1985), The Si:C:N ratio of marine diatoms: Interspecific variability and the effect of some environmental variables, *J. Phycol.*, *21*, 347–357.

Brzezinski, M. A., M. L. Dickson, D. M. Nelson, and R. Sambrotto (2003), Ratios of Si, C and N uptake by microplankton in the Southern Ocean, *Deep Sea Res., Part II*, *50*(3–4), 619–633.

Cardinal, D., L. Y. Alleman, J. de Jong, K. Ziegler, and L. Andre (2003), Isotopic composition of silicon measured by multicollector plasma source mass spectrometry in dry plasma mode, *J. Anal. At. Spectrom.*, *18*(3), 213–218, doi:10.1039/B210109b.

Cardinal, D., L. Y. Alleman, F. Dehairs, N. Savoye, T. W. Trull, and L. Andre (2005), Relevance of silicon isotopes to Si-nutrient utilization and Si-source assessment in Antarctic, *Global Biogeochem. Cycles*, *19*, GB2007, doi:10.1029/2004GB002364.

Cardinal, D., N. Savoye, T. W. Trull, F. Dehairs, E. E. Kopczynska, F. Fripiat, J. L. Tison, and L. Andre (2007), Silicon isotopes in spring Southern Ocean diatoms: Large zonal changes despite homogeneity among size fractions, *Mar. Chem.*, *106*(1–2), 46–62, doi:10.1016/J.Marchem.2006.04.006.

Collins, L. G., C. S. Allen, J. Pike, D. A. Hodgson, K. Weckström, and G. Massé (2013), Evaluating highly branched isoprenoid (HBI) biomarkers as a novel Antarctic sea-ice proxy in deep ocean glacial age sediments, *Quat. Sci. Rev.*, *79*(0), 87–9, doi:10.1016/j.quascirev.2013.02.004.

Costa, E., R. B. Dunbar, K. A. Kryc, D. A. Mucciarone, S. Brachfeld, E. B. Roark, P. L. Manley, R. W. Murray, and A. Leventer (2007), Solar forcing and El Niño-Southern Oscillation (ENSO) influences on productivity cycles interpreted from a late-Holocene high-resolution marine sediment record, Adélie Drift, East Antarctic Margin, *U.S. Geol. Surv. Nat. Acad. Short Res. Pap.*, *1047*(036), doi:10.3133/of2007-1047.srp036.

Cozzi, S., and C. Cantoni (2011), Stable isotope (δ^{13}C and δ^{15}N) composition of particulate organic matter, nutrients and dissolved organic matter during spring ice retreat at Terra Nova Bay, *Antarct. Sci.*, *23*(1), 43–56.

Crosta, X., and A. Shemesh (2002), Reconciling down core anticorrelation of diatom carbon and nitrogen isotopic ratios from the Southern Ocean, *Paleoceanography*, *17*(1), 1010, doi:10.1029/2000PA000565.

Crosta, X., A. Shemesh, M. E. Salvignac, H. Gildor, and R. Yam (2002), Late quaternary variations of elemental ratios (C/Si and N/Si) in diatom-bound organic matter from the Southern Ocean, *Deep Sea Res., Part II*, *49*(9–10), 1939–1952, doi:10.1016/S0967-0645(02)00019-X.

Crosta, X., J. Crespin, I. Billy, and O. Ther (2005), Major factors controlling Holocene $^{13}C_{org}$ changes in a seasonal sea-ice environment, Adelie Land, East Antarctica, *Global Biogeochem. Cycles*, *19*, GB4029, doi:10.1029/2004GB002426.

Crosta, X., M. Debret, D. Denis, M. A. Courty, and O. Ther (2007), Holocene long- and short-term climate changes off Adélie Land, East Antarctica, *Geochem. Geophys. Geosyst.*, *8*, Q11009 doi:10.1029/2007GC001718.

Crosta, X., D. Denis, and O. Ther (2008), Sea ice seasonality during the Holocene, Adélie Land, East Antarctica, *Mar. Micropaleontol.*, *66*(3–4), 222–232, doi:10.1016/J.Marmicro.2007.10.001.
De La Rocha, C. L., M. A. Brzezinski, and M. J. DeNiro (1997), Fractionation of silicon isotopes by marine diatoms during biogenic silica formation, *Geochim. Cosmochim. Acta*, *61*(23), 5051–5056, doi:10.1016/s0016-7037(97)00300-1.
De La Rocha, C. L., M. A. Brzezinski, M. J. DeNiro, and A. Shemesh (1998), Silicon-isotope composition of diatoms as an indicator of past oceanic change, *Nature*, *395*(6703), 680–683.
Denis, D., X. Crosta, S. Zaragosi, O. Romero, B. Martin, and V. Mas (2006), Seasonal and subseasonal climate changes recorded in laminated diatom ooze sediments, Adelie Land, East Antarctica, *Holocene*, *16*(8), 1137–1147.
Denis, D., et al. (2009a), Holocene glacier and deep water dynamics, Adélie Land region, East Antarctica, *Quat. Sci. Rev.*, *28*(13–14), 1291–1303.
Denis, D., X. Crosta, S. Schmidt, D. S. Carson, R. S. Ganeshram, H. Renssen, J. Crespin, O. Ther, I. Billy, and J. Giraudeau (2009b), Holocene productivity changes off Adélie Land (East Antarctica), *Paleoceanography*, *24*, PA3207, doi:10.1029/2008PA001689.
Denis, D., X. Crosta, L. Barbara, G. Masse, H. Renssen, O. Ther, and J. Giraudeau (2010), Sea ice and wind variability during the Holocene in East Antarctica: Insight on middle-high latitude coupling, *Quat. Sci. Rev.*, *29*(27–28), 3709–3719, doi:10.1016/J.Quascirev.2010.08.007.
Egan, K. E., R. E. M. Rickaby, M. J. Leng, K. R. Hendry, M. Hermoso, H. J. Sloane, H. Bostock, and A. N. Halliday (2012), Diatom silicon isotopes as a proxy for silicic acid utilisation: A Southern Ocean core top calibration, *Geochim. Cosmochim. Acta*, *96*, 174–192, doi:10.1016/j.gca.2012.08.002.
Fiala, M., H. Kuosa, E. E. Kopczynska, L. Oriol, and D. Delille (2006), Spatial and seasonal heterogeneity of sea ice microbial communities in the first-year ice of Terre Adélie area (Antarctica), *Aquat. Microb. Ecol.*, *43*(1), 95–106.
Fripiat, F., D. Cardinal, J. L. Tison, A. Worby, and L. Andre (2007), Diatom-induced silicon isotopic fractionation in Antarctic sea ice, *J. Geophys. Res. 112*, G02001, doi:10.1029/2006JG000244.
Fripiat, F., A.-J. Cavagna, N. Savoye, F. Dehairs, L. Andre, and D. Cardinal (2011), Isotopic constraints on the Si-biogeochemical cycle of the Antarctic Zone in the Kerguelen area (KEOPS), *Mar. Chem.*, *123*(1-4), 11–22, doi:10.1016/j.marchem.2010.08.005.
Gall, M. P., P. W. Boyd, J. Hall, K. A. Safi, and H. Chang (2001), Phytoplankton processes. Part 1: Community structure during the Southern Ocean Iron RElease Experiment (SOIREE), *Deep Sea Res., Part II*, *48*, 2551–2570.
Georg, R. B., B. C. Reynolds, M. Frank, and A. N. Halliday (2006), New sample preparation techniques for the determination of Si isotopic compositions using MC-ICPMS, *Chem. Geol.*, *235*(1-2), 95–104, doi:10.1016/J.Chemgeo.2006.06.006.
Gibson, J. A. E., T. Trull, P. D. Nichols, R. E. Summons, and A. McMinn (1999), Sedimentation of ^{13}C-rich organic matter from Antarctic sea-ice algae: A potential indicator of past sea-ice extent, *Geology*, *27*(4), 331–334, doi:10.1130/0091-7613(1999)027.
Hodell, D. A., S. L. Kanfoush, A. Shemesh, X. Crosta, C. D. Charles, and T. P. Guilderson (2001), Abrupt cooling of Antarctic surface waters and sea ice expansion in the South Atlantic sector of the Southern Ocean at 5000 cal yr B.P, *Quat. Res.*, *56*(2), 191–198, doi:10.1006/Qres.2001.2252.
Horn, M. G., C. P. Beucher, R. S. Robinson, and M. A. Brzezinski (2011), Southern Ocean nitrogen and silicon dynamics during the last deglaciation, *Earth Planet. Sci. Lett.*, *310*(3–4), 334–339, doi:10.1016/j.epsl.2011.08.016.
Hughen, K. A., et al. (2004), Marine04 marine radiocarbon age calibration, 0–26 cal kyr BP, *Radiocarbon*, *46*, 1059–1086.
Ingolfsson, O., C. Hjort, P. A. Berkman, S. Björck, and E. Colhoun (1998), Antarctic glacial history since the Last Glacial Maximum: An overview of the record on land, *Antarct. Sci.*, *10*(3), 326–344.
Jacot Des Combes, H., O. Esper, C. L. De La Rocha, A. Abelmann, R. Gersonde, R. Yam, and A. Shemesh (2008), Diatom δ^{13}C, δ^{15}N and C/N since the Last Glacial Maximum in the Southern Ocean: Potential impact of species composition, *Paleoceanography*, *23*, PA4209, doi:10.1029/2008PA001589.
Juillet-Leclerc, A., and L. D. Labeyrie (1987), Temperature dependance of the oxygen isotopic fractionation between diatom silica and water, *Earth Planet. Sci. Lett.*, *84*, 69–74.
Kennedy, H., D. N. Thomas, G. Kattner, C. Haas, and G. S. Dieckmann (2002), Particulate organic matter in Antarctic summer sea ice: Concentration and stable isotopic composition, *Mar. Ecol. Prog. Ser.*, *238*, 1–13, doi:10.3354/Meps238001.
Kim, J.-H., X. Crosta, V. Willmott, H. Renssen, J. Bonnin, P. Helmke, S. Schouten, and J. S. Damste (2012), Holocene subsurface temperature variability in the eastern Antarctic margin, *Geophys. Res. Lett.*, *39*, L06705, doi:10.1029/2012GL051157.
Leventer, A. (1992), Modern distribution of diatoms in sediments from the George-V-Coast, Antarctica, *Mar. Micropaleontol.*, *19*(4), 315–332, doi:10.1016/0377-8398(92)90036-J.
Leventer, A. (2003), Particulate flux from sea ice in polar waters, in *Sea Ice: An Introduction to its Physics, Biology, Chemistry and Geology*, edited by D. N. Thomas and G. S. Dieckmann, pp. 333–372, Blackwell Science Ltd., Oxford, U. K.
Lizotte, M. P. (2001), The contributions of sea ice algae to Antarctic marine primary production, *Am. Zool.*, *41*(1), 57–73.
Martin, J. H. (1990), Glacial-interglacial CO_2 change: The iron hypothesis, *Paleoceanography*, *5*(1), 1–13, doi:10.1029/Pa005i001p00001.
Martin, J. H., and S. E. Fitzwater (1988), Iron-deficiency limits phytoplankton growth in the northeast Pacific subarctic, *Nature*, *331*(6154), 341–343, doi:10.1038/331341a0.
Martin, J. H., and R. M. Gordon (1988), Northeast Pacific iron distributions in relation to phytoplankton productivity, *Deep Sea Res., Part A*, *35*(2), 177–196, doi:10.1016/0198-0149(88)90035-0.
Martin, J. H., W. W. Broenkow, S. E. Fitzwater, and R. M. Gordon (1990a), Does iron really limit phytoplankton production in the offshore sub-Arctic Pacific - Yes, it does - A reply, *Limnol. Oceanogr.*, *35*(3), 775–777.
Martin, J. H., R. M. Gordon, and S. E. Fitzwater (1990b), Iron in Antarctic waters, *Nature*, *345*(6271), 156–158.
Massé, G., S. T. Belt, X. Crosta, S. Schmidt, I. Snape, D. N. Thomas, and S. J. Rowland (2011), Highly branched isoprenoids as proxies for variable sea ice conditions in the Southern Ocean, *Antarct. Sci.*, *23*(5), 487–498, doi:10.1017/s0954102011000381.
Masson, V., et al. (2000), Holocene climate variability in Antarctica based on 11 ice-core isotopic records, *Quat. Res.*, *54*, 348–358.
Masson-Delmotte, V., B. Stenni, and J. Jouzel (2004), Common millennial-scale variability of Antarctic and Southern Ocean temperatures during the past 5000 years reconstructed from EPICA Dome C ice core, *Holocene*, *14*, 145–151.
Mathiot, P., H. Goosse, X. Crosta, B. Stenni, M. Braida, H. Renssen, C. J. Van Meerbeeck, V. Masson-Delmotte, A. Mairesse, and S. Dubinkina (2013), Using data assimilation to investigate the causes of Southern Hemisphere high latitude cooling from 10 to 8 ka BP, *Clim. Past*, *9*(2), 887–901, doi:10.5194/cp-9-887-2013.
Matsumoto, K., J. L. Sarmiento, and M. A. Brzezinski (2002), Silicic acid leakage from the Southern Ocean: A possible explanation for glacial atmospheric pCO_2, *Global Biogeochem. Cycles*, *16*(3), 1031, doi:10.1029/2001GB001442.
McMinn, A., J. Skerratt, T. Trull, C. Ashworth, and M. Lizotte (1999), Nutrient stress gradient in the bottom 5 cm of fast ice, McMurdo Sound, Antarctica, *Polar Biol.*, *21*(4), 220–227, doi:10.1007/S003000050356.
Michels, J., G. S. Dieckmann, D. N. Thomas, S. B. Schnack-Schiel, A. Krell, P. Assmy, H. Kennedy, S. Papadimitriou, and B. Cisewski (2008), Short-term biogenic particle flux under late spring sea ice in the western Weddell Sea, *Deep Sea Res., Part II*, *55*, 1024–1039, doi:10.1016/j.dsr2.2007.12.019.

Milligan, A. J., D. E. Varela, M. A. Brzezinski, and F. O. M. M. Morel (2004), Dynamics of silicon metabolism and silicon isotopic discrimination in a marine diatom as a function of pCO_2, *Limnol. Oceanogr.*, *49*(2), 322–329.
Mills, M. M., A.-C. Alderkamp, C.-E. Thuroczy, G. L. van Dijken, P. Laan, H. J. W. de Baar, and K. R. Arrigo (2012), Phytoplankton biomass and pigment responses to Fe amendments in the Pine Island and Amundsen polynyas, *Deep Sea Res., Part II*, *71–76*, 61–76, doi:10.1016/j.dsr2.2012.03.008.
Morley, D. W., M. J. Leng, A. W. Mackay, H. J. Sloane, P. Rioual, and M. Sturm (2004), Cleaning of lake sediment samples for diatom oxygen isotope analysis, *J. Paleolimnol.*, *31*, 391–401.
Munro, D. R., R. B. Dunbar, D. A. Mucciarone, K. R. Arrigo, and M. C. Long (2010), Stable isotope composition of dissolved inorganic carbon and particulate organic carbon in sea ice from the Ross Sea, Antarctica, *J. Geophys. Res.*, *115*, C09005, doi:10.1029/2009JC005661.
Nelson, D. M., P. Treguer, M. A. Brzezinski, A. Leynaert, and B. Queguiner (1995), Production and dissolution of biogenic silica in the ocean - Revised global estimates, comparison with regional data and relationship to biogenic sedimentation, *Global Biogeochem. Cycles*, *9*(3), 359–372, doi:10.1029/95GB01070.
Papadimitriou, S., D. N. Thomas, H. Kennedy, C. Haas, H. Kuosa, A. Krell, and G. S. Dieckmann (2007), Biogeochemical composition of natural sea ice brines from the Weddell Sea during early austral summer, *Limnol. Oceanogr.*, *52*(5), 1809–1823, doi:10.4319/Lo.2007.52.5.1809.
Papadimitriou, S., D. N. Thomas, H. Kennedy, H. Kuosa, and G. S. Dieckmann (2009), Inorganic carbon removal and isotopic enrichment in Antarctic sea ice gap layers during early austral summer, *Mar. Ecol. Prog. Ser.*, *386*, 15–27, doi:10.3354/Meps08049.
Pichevin, L., R. S. Ganeshram, B. C. Reynolds, F. Prahl, T. F. Pedersen, R. Thunell, and E. L. McClymont (2012), Silicic acid biogeochemistry in the Gulf of California: Insights from sedimentary Si isotopes, *Paleoceanography*, *27*, PA2201, doi:10.1029/2011PA002237.
Pondaven, P., O. Ragueneau, P. Treguer, A. Hauvespre, L. Dezileau, and J. L. Reyss (2000), Resolving the 'opal paradox' in the Southern Ocean, *Nature*, *405*(6783), 168–172, doi:10.1038/35012046.
Rau, G. H., C. W. Sullivan, and L. I. Gordon (1991), $\delta^{13}C$ and $\delta^{15}N$ variations in Weddell Sea particulate organic-matter, *Mar. Chem.*, *35*(1–4), 355–369.
Renssen, H., H. Goosse, T. Fichefet, V. Masson-Delmotte, and N. Koc (2005), Holocene climate evolution in the high-latitude Southern Hemisphere simulated by a coupled atmosphere-sea ice-ocean-vegetation model, *Holocene*, *15*(7), 951–964, doi:10.1191/0959683605hl869ra.
Reynolds, B. C., et al. (2007), An inter-laboratory comparison of Si isotope reference materials, *J. Anal. At. Spectrom.*, *22*, 561–568.
Rosenthal, Y., M. Dahan, and A. Shemesh (2000), Southern Ocean contributions to glacial-interglacial changes of atmospheric pCO_2: An assessment of carbon isotope records in diatoms, *Paleoceanography*, *15*(1), 65–75, doi:10.1029/1999PA000369.
Sambrotto, R. N., A. Matsuda, R. Vaillancourt, M. Brown, C. Langdon, S. S. Jacobs, and C. Measures (2003), Summer plankton production and nutrient consumption patterns in the Mertz Glacier Region of East Antarctica, *Deep Sea Res., Part II*, *50*(8–9), 1393–1414, doi:10.1016/S0967-0645(03)00076-6.
Sarmiento, J. L., N. Gruber, M. A. Brzezinski, and J. P. Dunne (2004), High-latitude controls of thermocline nutrients and low latitude biological productivity, *Nature*, *427*(6969), 56–60, doi:10.1038/Nature02127.
Scharek, R. M., M. A. van Leeuwe, and H. J. W. de Baar (1997), Responses of Southern Ocean phytoplankton to the addition of trace metals, *Deep Sea Res., Part II*, *44*, 209–227.
Schneider-Mor, A., R. Yam, C. Bianchi, M. Kunz-Pirrung, R. Gersonde, and A. Shemesh (2005), Diatom stable isotopes, sea ice presence and sea surface temperature records of the past 640 ka in the Atlantic sector of the Southern Ocean, *Geophys. Res. Lett.*, *32*, L10704, doi:10.1029/2005GL022543.
Schneider-Mor, A., R. Yam, C. Bianchi, M. Kunz-Pirrung, R. Gersonde, and A. Shemesh (2008), Nutrient regime at the siliceous belt of the Atlantic sector of the Southern Ocean during the past 660 ka, *Paleoceanography*, *23*, PA3217, doi:10.1029/2007PA001466.
Schweitzer, P. N. (1995), *Monthly Average Polar Sea-ice Concentration*, U.S. Geological Survey Digital Data Series, vol. DDS-27, U.S. Geol. Surv. Digital Data, Reston, Virginia.
Sedwick, P., G. R. DiTullio, and D. J. Mackey (2000), Iron and manganese in the Ross Sea, Antarctica: Seasonal iron limitation in Antarctic shelf waters, *J. Geophys. Res.*, *105*(C5), 11,321–11,336.
Shemesh, A., S. A. Macko, C. D. Charles, and G. H. Rau (1993), Isotopic evidence for reduced productivity in the glacial Southern-Ocean, *Science*, *262*(5132), 407–410, doi:10.1126/Science.262.5132.407.
Shemesh, A., L. H. Burckle, and J. D. Hays (1995), Late Pleistocene oxygen-isotope records of biogenic silica from the Atlantic sector of the Southern-Ocean, *Paleoceanography*, *10*(2), 179–196, doi:10.1029/94PA03060.
Shemesh, A., D. Hodell, X. Crosta, S. Kanfoush, C. Charles, and T. Guilderson (2002), Sequence of events during the last deglaciation in Southern Ocean sediments and Antarctic ice cores, *Paleoceanography*, *17*(4), 1056, doi:10.1029/2000PA000599.
Singer, A. J., and A. Shemesh (1995), Climatically linked carbon-isotope variation during the past 430,000 years in Southern-Ocean sediments, *Paleoceanography*, *10*(2), 171–177, doi:10.1029/94PA03319.
Smetacek, V. (1998), Diatoms and the silicate factor, *Nature*, *391*, 224–225.
Smetacek, V., P. Assmy, and J. Henjes (2004), The role of grazing in structuring Southern Ocean pelagic ecosystems and biogeochemical cycles, *Antarct. Sci.*, *16*(4), 541–558, doi:10.1017/s0954102004002317.
Smith, W. O., and L. I. Gordon (1997), Hyperproductivity of the Ross Sea (Antarctica) polynya during austral spring, *Geophys. Res. Lett.*, *24*(3), 233–236, doi:10.1029/96GL03926.
Stuiver, M., et al. (2005), CALIB 5.0.
Sutton, J. N., D. E. Varela, M. A. Brzezinski, and C. P. Beucher (2013), Species-dependent silicon isotope fractionation by marine diatoms, *Geochim. Cosmochim. Acta*, *104*, 300–309, doi:10.1016/J.Gca.2012.10.057.
Takeda, S. (1998), Influence of iron availability on nutrient consumption ratio of diatoms in oceanic waters, *Nature*, *393*, 774–777.
Thomas, D. N., and A. Papadimitriou (2003), Biogeochemistry of sea ice, in *Sea Ice: An Introduction to its Physics, Chemistry, Biology and Geology*, edited by D. N. Thomas and G. S. Dieckmann, pp. 267–303, Blackwell Science, Oxford.
Thomas, D. N., H. Kennedy, G. Kattner, D. Gerdes, C. Gough, and G. S. Dieckmann (2001), Biogeochemistry of platelet ice: Its influence on particle flux under fast ice in the Weddell Sea, Antarctica, *Polar Biol.*, *24*(7), 486–496, doi:10.1007/S003000100243.
Thuróczy, C.-E., A.-C. Alderkamp, P. Laan, L. J. A. Gerringa, M. M. Mills, G. L. Van Dijken, H. J. W. De Baar, and K. R. Arrigo (2012), Key role of organic complexation of iron in sustaining phytoplankton blooms in the Pine Island and Amundsen Polynyas (Southern Ocean), *Deep Sea Res., Part II*, *71–76*, 49–60, doi:10.1016/j.dsr2.2012.03.009.
Varela, D. E., C. J. Pride, and M. A. Brzezinski (2004), Biological fractionation of silicon isotopes in Southern Ocean surface waters, *Global Biogeochem. Cycles*, *18*, GB1047, doi:10.1029/2003GB002140.
Villinski, J. C., R. B. Dunbar, and D. A. Mucciarone (2000), Carbon 13/Carbon 12 ratios of sedimentary organic matter from the Ross Sea, Antarctica: A record of phytoplankton bloom dynamics, *J. Geophys. Res.*, *105*(C6), 14,163–14,172, doi:10.1029/1999JC000309.

Weston, K., T. D. Jickells, D. S. Carson, A. Clarke, M. P. Meredith, M. A. Brandon, M. I. Wallace, S. J. Ussher, and K. R. Hendry (2013), Primary production export flux in Marguerite Bay (Antarctic Peninsula): Linking upper water-column production to sediment trap flux, *Deep Sea Res., Part I*, *75*, 52–66, doi:10.1016/j.dsr.2013.02.001.

Wright, S. W., and R. L. van den Enden (2000), Phytoplankton community structure and stocks in the East Antarctic Marginal ice zone (BOKE survey, January-March 996), *Deep Sea Res., Part II*, *47*, 2363–2400.

Young, E. D., A. Galy, and H. Nagahara (2002), Kinetic and equilibrium mass-dependent isotope fractionation laws in nature and their geochemical and cosmochemical significance, *Geochim. Cosmochim. Acta*, *66*(6), 1095–1104.